NJC

ROYAL SOCIETY OF CHEMISTRY

PAPER

View Article Online
View Journal | View Issue

Cite this: *New J. Chem.*, 2023, **47**, 8515

Binaphthalene-based cyclic homochiral ureas and their structure-related properties†

Roman Holakovský,[a] David Just,[a] Václav Eigner,[a] Martin Jakubec[b] and Petra Cuřínová *[ab]

Received 16th December 2022,
Accepted 29th March 2023

DOI: 10.1039/d2nj06147c

rsc.li/njc

Enantiomeric purity control is a must when working with chiral drugs. In this context, homochiral cycles consisting solely of 1 to 3 binaphthalene units interconnected with urea moieties were tested as chiral solvating agents for enantiomers of naproxen. Among the tested compounds, only the dimeric structure formed stable diastereomeric complexes with naproxen with K_R = 43 ± 3 M^{-1}/K_S = 34 ± 2 M^{-1}. When the conformational mobility of the dimer was decelerated by cooling to −30 °C, the complexes became stronger ($K_{R\text{-}30}$ = 100 ± 6 M^{-1}/$K_{S\text{-}30}$ = 102 ± 7 M^{-1}). Using DFT calculations, the probable structures of the diastereomeric complex were proposed.

Introduction

Systems based on the structural constituent of binaphthalene have gained indisputable popularity in the field of chiral recognition due to their robustness, stability, and easy resolution of enantiomers.[1,2] Thanks to these properties, the binaphthalene moiety has become a reasonable choice in efforts to incorporate chirality into intended enantioselective hosts. To date, many binaphthalene-based chiral receptors have been studied and published, recognizing, among others, enantiomers of aminoacids,[3,4] saccharides,[5] sulfoxides,[6] alcohols,[7] and arylpropanoic acids.[8] A special class of binaphthalene-based receptors is represented by cyclic structures, which introduce an additional structural feature beneficial for enantioseparation – conformational rigidity. For this reason, several macrocycles containing two binaphthalene units connected by various spacers were obtained, with cavities differing in both shape and size.[9–11] Although not used for chiral recognition, some of them were able to recognize achiral dicarboxylates, with a preference for glutarate over succinate.

Hydrogen bonding towards the ureido moiety of the host is often employed to coordinate guests containing carboxylic functionality.[12,13] This type of binding site provides a highly directional interaction, which is beneficial for prediction of the structure of the resulting complex. Using this complexation site in cyclic bischromenylureas resulted in the formation of an effective receptor of hydroxyacids.[14] A similar bischromenylureido motif was applied in the synthesis of a rigid host for naproxenate discriminating the *R* enantiomer with an enantioselectivity factor (K_R/K_S) = 7.2.[15] Cyclic receptors containing both the bischromenylurea moiety and the binaphthalene group were used in chiral recognition of amino acid enantiomers.[16] The connection of the urea moiety and axially chiral binaphthalene was also used for the synthesis of a highly enantioselective cyclic receptor with a very small cavity, which discriminates 2-phenylbutylate guests with an enantioselectivity factor K_R/K_S = 5.[17]

In our previous work we investigated the possibility of using ureido-1,1′-binaphthalenes as solvating agents for arylpropanoic acids. (S_a)-2,2′-bis[*N*,*N*′-bis(phenyl]ureido-1,1′-binaphthalene (**P1**, Fig. 1) bound enantiomers of ibuprofen with K_R = 110 ± 2 M^{-1}/K_S = 115 ± 5 M^{-1}, and, despite the similar values of binding constants, the particular diastereomeric complexes were easily distinguishable in the ^{1}H NMR spectra. In the present work we aim to synthesize its cyclic analogues using the direct connection of binaphthalene units with urea moieties. We investigate the cyclization-based change of properties of thus obtained homochiral compounds especially in terms of conformational preferences and accordingly in terms of naproxen binding. Moreover, we attempt to solve the structure of the diastereomeric complexes with naproxen to get better insight into the background of their possible chiral solvating function.

Results and discussion

Synthesis

Addition of 1 equiv. of triphosgene into the pyridine solution of (S_a)-1,1′-binaphthalene-2,2′-diamine **4** leads to the formation of cyclic structures with a variable number of binaphthalene moieties. The resulting reaction mixture consists mainly of

[a] *University of Chemistry and Technology Prague, Technická 5, 166 28 Prague 6, Praha, Czech Republic. E-mail: Petra.Curinova@vscht.cz*
[b] *Institute of Chemical Process Fundamentals of CAS, v.v.i, Rozvojová 135, 165 02 Prague 6, Praha, Czech Republic*

† Electronic supplementary information (ESI) available. CCDC 2226943 and 2226944. For ESI and crystallographic data in CIF or other electronic format see DOI: https://doi.org/10.1039/d2nj06147c

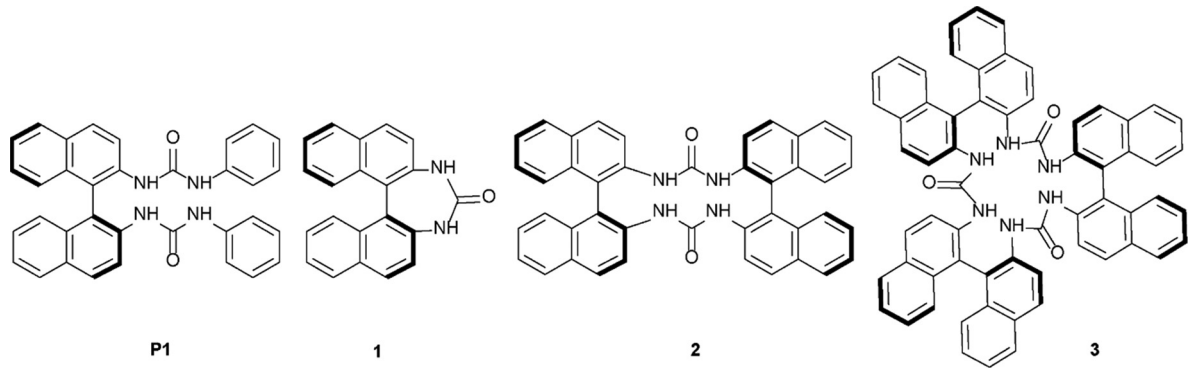

Fig. 1 Structures of compounds **1–3** and of a previously prepared compound **P1**.[8]

the smallest cycle **1**, which can be isolated as a white solid. The remainder of the obtained material consists predominantly of **2**. According to the HRMS analysis, larger cyclic oligomers like trimer **3** and even larger cycles were also present in small amounts but could not be isolated from the reaction mixture (Fig. 1 and Scheme 1 and Fig. S19, ESI†).

In order to obtain compound **2** selectively, a stepwise synthetic protocol was followed, including the additional step of formation of bis(isocyanate) **5** (Scheme 1). Compound **5** was formed by the addition of excess of phosgene (solution in toluene) to 1,1′-binaphthalene-2,2′-diamine **4** in the presence of pyridine. The simultaneous addition of 1,1′-binaphthalene diamine **4** and compound **5** into a reaction vessel filled with toluene resulted in the formation of **2** in 70% yield. The targeted synthesis of **3** was somewhat more difficult. The starting compound was monoprotected with benzyl chloroformate (Z-Cl) according to a known procedure.[16] Subsequent reaction of Z-protected product **6** with excess of phosgene gave isocyanate **7**. The reaction of **7** with amine **6** resulted in dimer **8**. Deprotection led to diamino-derivative **9**, which in combination with diisocyanate **5** in toluene gave compound **3** in 52% yield.

Solution-state properties

^{1}H NMR spectra of the prepared receptors show interesting features. Compound **1** is scarcely soluble in chloroform, so the ^{1}H NMR spectrum was therefore measured in DMSO-d_6. The obtained spectrum contains seven signals, which indicates a symmetrical and stable conformation (Fig. S1, ESI†). Compared to acyclic ureido-1,1′-binaphthalenes,[6–8] the NH signals in **1** are significantly shifted to the lower field (9.03 ppm). This feature results from two factors: first, considering the steric demands of the seven-membered ring, the NH-hydrogens

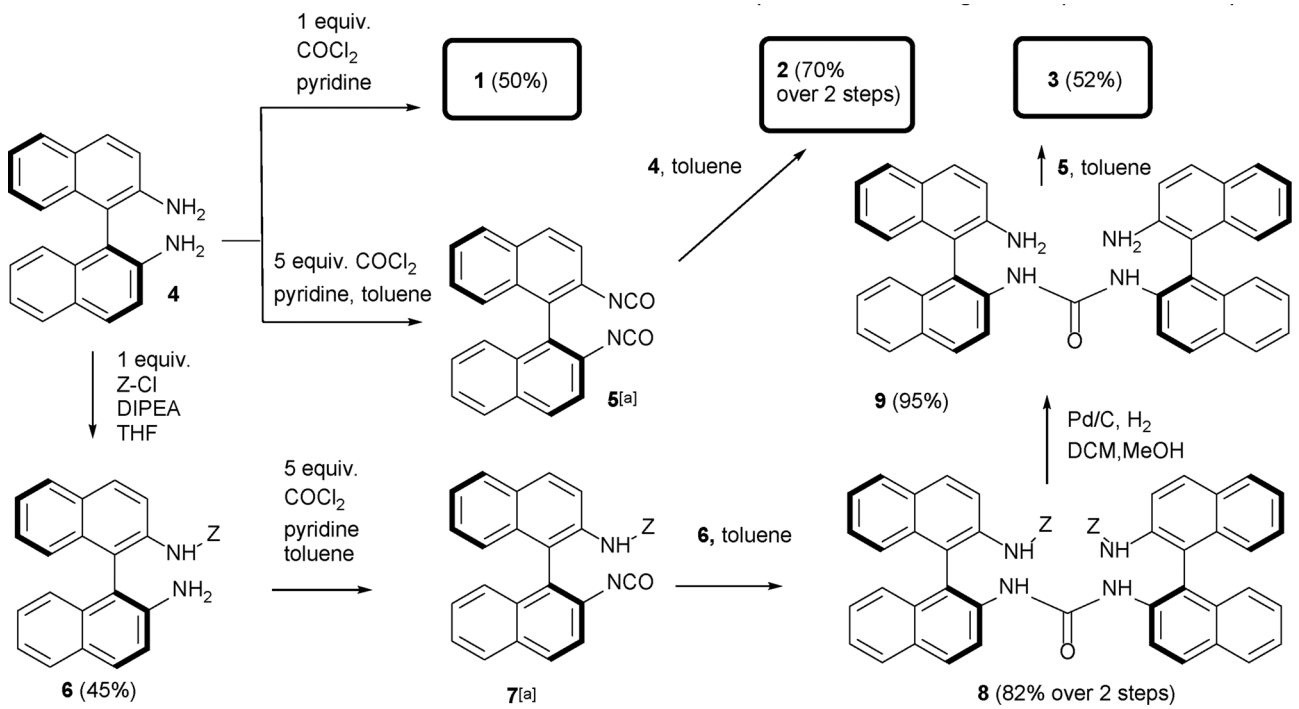

Scheme 1 Synthesis of compounds **1–3**. [a] not isolated, 100% conversion assumed.

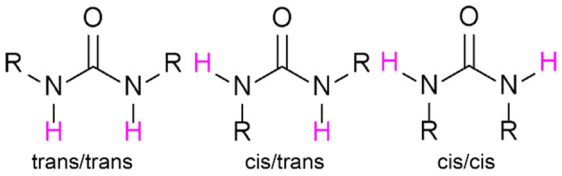

Fig. 2 Mutual position of NH-hydrogens in urea derivatives.

stretch out of the cycle in a so-called *cis*/*cis* arrangement[18] (Fig. 2). Moreover, compound **1** is here present as a complex with DMSO, with inclusion of NHs into hydrogen bonds. This complex can be disrupted at higher temperatures, where the formation of hydrogen bonds is more difficult due to higher structural mobility. With sequential heating of the sample, the position of the signal of NHs moves to the higher field (Fig. S21, ESI†).

In the case of **2**, one would expect D_2 symmetry, which is supported by twelve signals of aromatic protons in ^{1}H NMR (chloroform-d) spectrum (Fig. 3). However, the non-equivalency in NH groups leading to two different signals belonging to NHs indicates a somewhat more complicated conformation. Moreover, the ^{13}C NMR spectrum also shows non-equivalency in NH-attached quaternary carbons and proximal CHs (Fig. S6, ESI†). All these parameters are met only in the *cis*/*trans* NH conformation, reducing the symmetry of the molecule **2** to C_2. Here, the two *cis*-NHs are stretching out of the cavity of **2**, and the *trans*-NHs are embedded in the cavity of the macrocycle. The *cis*/*trans* orientation of NHs causes the moderate non-equivalency of the proximal hydrogens and concerned carbons and thus their broadening and splitting, respectively. As proven by exchange-based cross-peaks in 2D ROESY spectra (Fig. S11, ESI†), the observed ^{1}H NMR signals are broad due to conformational exchange; the *cis*-NH′ flips to *trans*-NH′, and at the same time the *trans*-NH″ becomes *cis*-NH″. The thus formed conformer″ has the same structure as conformer′, due to the symmetry. By heating in chloroform-*d*, the ^{1}H NMR signals gradually broaden. Cooling to 0 °C causes signal sharpening, and at −30 °C all the conformational changes are frozen (Fig. S13, ESI†). When dissolved in DMSO-d_6, compound **2** is present as a DMSO-complex with *cis*-NH proton shifted to the low field. On heating, the signals broaden, the molecule of DMSO is released from the complex due to the increased molecular dynamics of **2**, and the signal of *cis*-NH moves back to the higher field (Fig. S21, ESI†).

Macrocycle **3** has a very simple ^{1}H NMR (chloroform-*d*) spectrum, containing only seven signals (Fig. S14, ESI†). This implies the D_3 symmetry of the structure of **3** with *cis*/*trans* conformation of NH hydrogens. On the other hand, the presence of chirality reduces the symmetry to C_3 and the

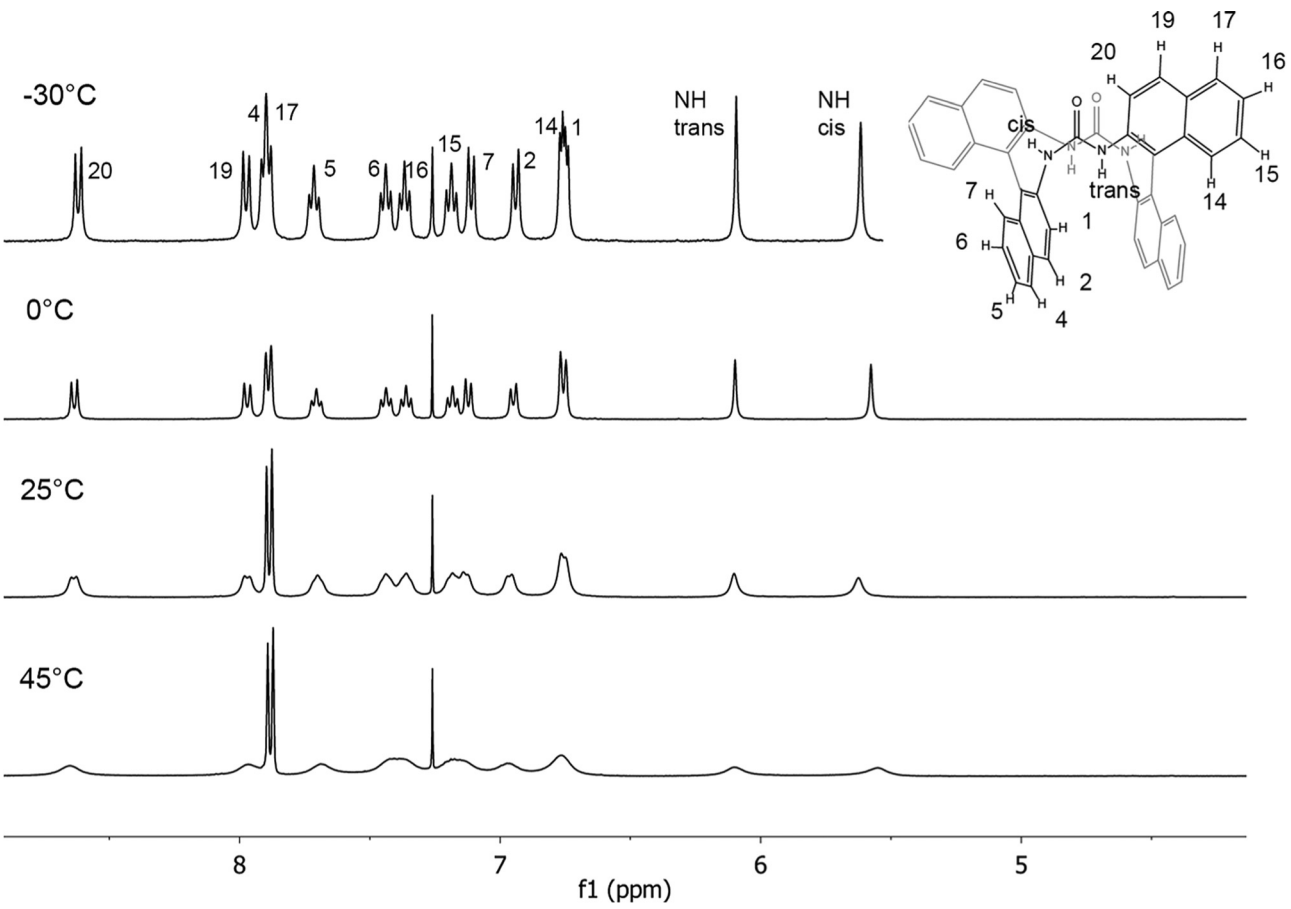

Fig. 3 ^{1}H NMR (chloroform-d) spectra of **2** at variable temperatures.

presence of only one set of signals can be more likely attributed to the molecular dynamic. In contrast to **2**, the ^{1}H NMR signals of **3** are rather sharp, except for the very broad signal of Ar-H 1 (atom numbering in Fig. 5). This broadening corresponds to the conformational equilibria at the ambient temperature; Ar–H 1, when proximal to *trans* NH, is very near to urea oxygen and can weakly interact with its lone electron pairs, while the same Ar–H 1, when proximal to *cis* NH, is free of this influence. The NH *cis*/*trans* interconversion at the urea group is rather quick at 25 °C, bringing the signals of Ar–H 1 near coalescence, while moderate heating (45 °C) causes coalescence completion and signal sharpening. On cooling, the signals highly broaden, stabilizing and thus making observable different possible conformations (Fig. S19, ESI†).

Solid-state properties

Compounds **1** and **2** provided single crystals suitable for X-ray crystallography, enabling the direct observation of the structural features in the solid state. The data obtained from X-ray diffraction measurement revealed the same conformation as observed in the solution. Compound **1** belongs to the C_2 symmetry point group (Fig. 4); the twisted conformation of the seven-membered cycle in **1** with each NH distorted in a way to form two planes with corresponding naphthyl complies with the demands of the two-fold rotational axis. Along this plane, each urea moiety provides hydrogen bonding to two other molecules, thus forming unidirectional chains of hydrogen-bound molecules, which explains the poor solubility of compound **1**. The conformation of **2** in the solid state also matches the shape expected after the solution study. Therefore, the difference in the position of ^{1}H NMR signals belonging to aromatic hydrogens proximal to urea moieties can be explained by the analysis of the crystal structure (Fig. 5a). While two of these hydrogens (Ar–H 20) are in close spatial proximity to urea oxygen exposed to its free electron pairs, the other two (Ar–H 1) are free from this influence.

Unfortunately, the attempts to obtain single crystals of **3** suitable for X-ray diffraction analysis failed. Based on the shape of binaphthalene moiety obtained for crystals of **1**, the shape of molecule **3** was calculated. The preferred *cis*/*trans* conformation of NH hydrogens was confirmed, and the D_3 symmetrical structure was verified as a possible conformation with minimal energy. According to computer assisted molecular modelling[18] as well as CSD (Cambridge Structural Database) mining, the preferred configuration of substituted ureas is *trans*/*trans*. Some examples of less populated *trans*/*cis* conformation can also be found,[19] usually caused by hydrogen bonding towards a suitable partner or to some other part of the molecule. In the solid state, the *cis*/*cis* conformation is very rare and is usually present only in cyclic derivatives.

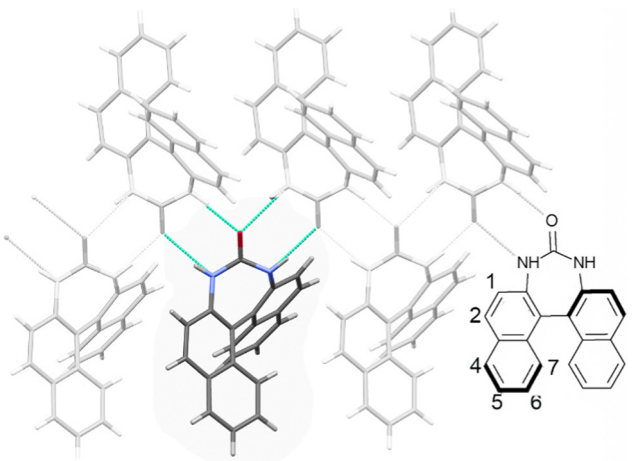

Fig. 4 Crystal structure of **1**.

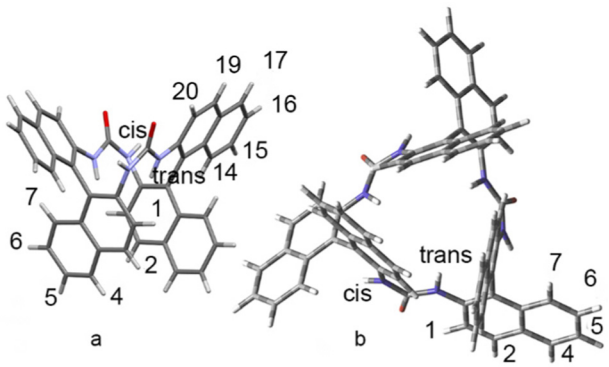

Fig. 5 Crystal structure of **2** (a) and calculated structure of **3** (b).

Complexation behaviour

The obtained homochiral compounds were originally intended to be used as chiral solvating agents forming diastereomeric complexes with chiral drugs, since these properties were found in their acyclic analogues.[8] In the case of cyclic ureas **1–3**, the complexation properties showed unexpected aspects caused by cyclization-based structural features. The structure of **1** with NHs in *cis*/*cis* conformation and possible di- or oligomerization causes the poor solubility of **1** in chloroform. The compound can be dissolved in DMSO, but this solvent highly competes with the carboxylic acid groups of targeted analytes, preventing the complexation.

Regarding the structure of macrocycle **2**, the mutual *cis*/*trans* position of NHs does not allow their synergistic cooperation in binding a substrate. Moreover, the strained structure causing permanent conformational changes makes the complexation less probable than for acyclic compounds. These hypotheses were tested using enantiomers of naproxen in a standard ^{1}H NMR titration[20,21] (Fig. 6). Aliquots of the solution of naproxen enantiomers were gradually added to the chloroform-d solution of **2**, and the shifts of the corresponding protons were monitored by ^{1}H NMR. The measurement revealed that only *cis*-NHs are complexation affected, and the changes in the position of *trans*-NHs are negligible (Fig. 6a, red peak). Moreover, the aromatic protons 17/4 (Fig. 6a, blue) corresponding to the sharp doublet at 7.88 ppm and 1/14 at 6.76 ppm (Fig. 6a, green) become magnetically non-equivalent in the naproxen complex, showing a more pronounced difference between the upper and lower part of **2**.

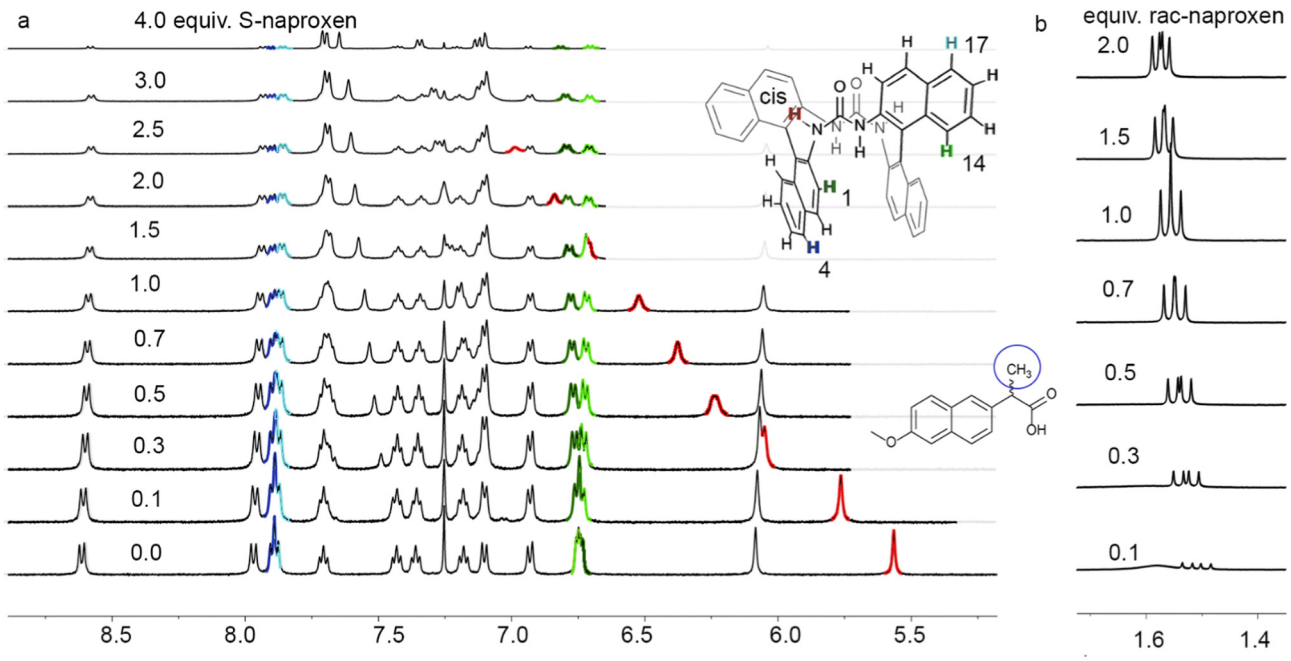

Fig. 6 ^{1}H NMR titration of **2** (chloroform-d): (a) with *S*-naproxen, −30 °C, and (b) with racemic naproxen, 25 °C, CH_3 signal splitting.

Fig. 6b shows the behaviour of naproxen CH_3 groups during the same experiment performed at 25 °C with racemic naproxen. In low loadings of naproxen, the well-separated signals of both diastereomeric complexes can be observed, which gradually become coalescent with the decrease of the molar fraction of receptor **2**. The diastereomeric complexes of **2** with naproxen enantiomers are not equivalent for NMR; except the hydrogens at the 3- and 4- position of naphthalene, all the naproxen protons are more magnetically shielded for S-enantiomer when working at the same **2**-to-naproxen ratio (Fig. S25, ESI†). However, the receptor affinity towards both enantiomers is practically the same (K_R = 43 ± 3 M^{-1}/K_S = 34 ± 2 M^{-1}).[22] The low association constants at ambient temperature are caused by the dynamic mode of naproxen binding; the complexes become stronger at −30 °C ($K_{R\text{-}30}$ = 100 ± 6 M^{-1}/$K_{S\text{-}30}$ = 102 ± 7 M^{-1}), where the conformational changes of **2** are blocked.

The structure of the complex was solved with the help of 2D NMR ROESY spectra measured at −30 °C, where the

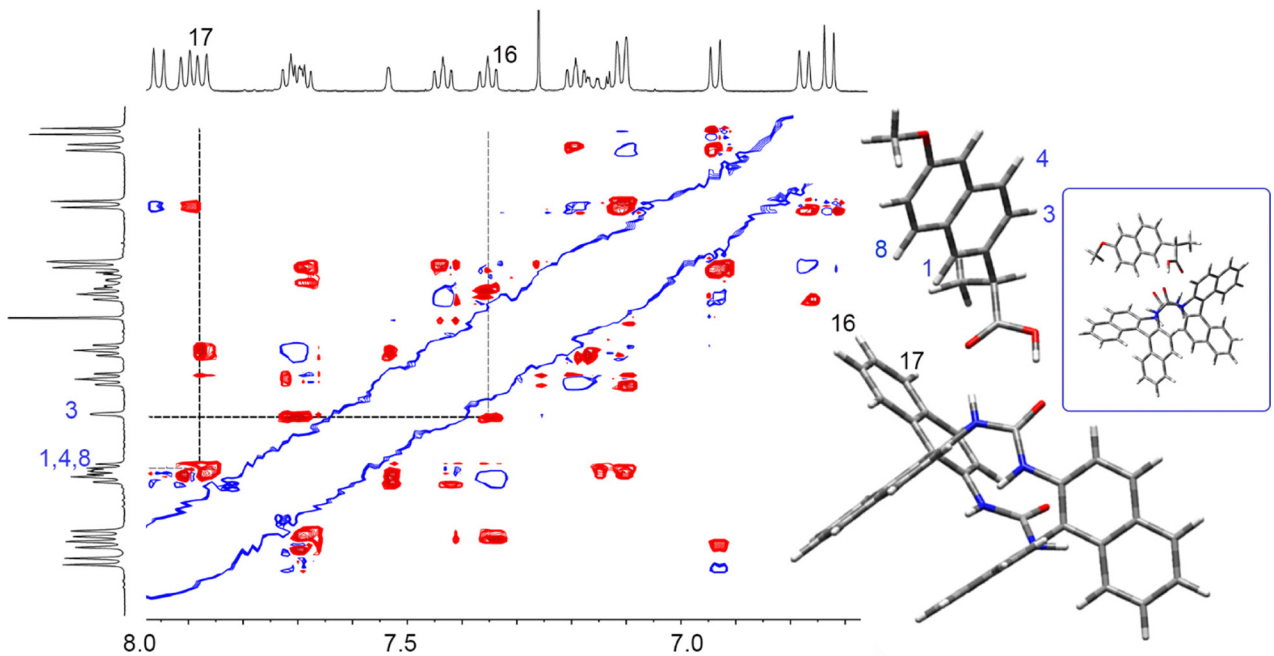

Fig. 7 2D ROESY spectrum of *S*-naproxen complex with **2**. The possible calculated structures of the complex are shown.

conformational exchange in **2** is minimal. Although the aromatic region of the spectra is very crowded, the cross-peaks showing the spatial proximity of **2**-Ar–H 16 with *S*-naproxen Ar–H at position 3 and **2**-Ar–H 17 with naproxen Ar–H at positions 1, 4 and 8 are clearly visible (Fig. 7 and Fig. S23, ESI†). Accordingly, the possible structures of the complex were calculated by computer-assisted modelling. The bigger structure at Fig. 7 with naproxen molecule interacting with CO and NH groups belonging to the same urea moiety is 1.7 kcal mol^{-1} more probable than the small one, where naproxen molecule bridges the cavity of **2** and interacts with CO and NH groups belonging to different urea moieties. However, going from −30 °C to the ambient temperature, the complexation process in this system becomes very dynamic with ROESY spectra full of exchange peaks, preventing a responsible readout of intermolecular interactions (Fig. S24, ESI†).

The complexation of a carboxylic acid function by a single urea group should be highlighted here as rare and requiring the said blocking of the *cis*/*trans* conformation of the urea moiety. In the compounds of **P1**-type (Fig. 1), carboxylic acid is bound to both urea moieties, one functioning as a hydrogen bond donor and the second one as a hydrogen bond acceptor. The change of one urea group in **P1** to aminoethyl means that one of the interactions is lost and naproxen is not bound at all, although binding towards a single ureido moiety is still theoretically possible.[8] On the other hand, in the literature, the examples of a single ureido moiety functioning at the same time as hydrogen bond donor and acceptor can be found, but the *cis*/*trans* conformation is always blocked, for example, by hydrogen-bonding towards some other structural feature of the receptor molecule,[23] or being a part of uracil-like structures.[24]

Receptor **3** possesses three ureido moieties available for naproxen binding and a larger, more flexible cavity. Accordingly, the naproxen molecule is bound in a very dynamic mode and with unclear stoichiometry. Addition of aliquots of racemic naproxen solution causes moderate changes in the NH-signal position and further broadening of proximal Ar–H. However, the properties of chiral shifting agent are lost, and only very moderate splitting of naproxen signals can be observed at low loadings (Fig. S31, ESI†).

Experimental

General

The reagents were purchased from commercial sources and used without further purification. Anhydrous solvents, toluene and THF were dried using a Pure-Solv MD7 solvent drying line (Innovative Technology, USA), pyridine was stored above NaOH(s). The ^{1}H (400 MHz) and ^{13}C (101 MHz) NMR spectra were recorded using a Bruker Avance 400 spectrometer at 25 °C (Bruker, Germany) and ^{1}H (500 MHz) and ^{1}H-^{1}H ROESY (500 MHz) NMR spectra at −30 °C on an Agilent 500 (Agilent, USA) spectrometer. Used solvents (DMSO-d_6, chloroform-d) were stored over molecular sieves. The ^{1}H and ^{13}C NMR spectra were referenced to the line of the solvent (δ/ppm; δ_H/δ_C: DMSO-d_6, 2.50/39.52, chloroform-*d*, 7.26/77.16). To assign all proton and carbon signals, a combination of 1D and 2D experiments (H,C-HSQC, H,C-HMBC, TOCSY and ROESY) was used. The high-resolution mass spectra (HRMS) were measured using a MicrOtof III spectrometer (Bruker, Germany) with an electrospray (ESI) ionization source in positive mode. For calibration of accurate masses, ESI-APCI Low Concentration Tuning Mix (Agilent) was used. Diffraction data were collected on a Rigaku OD Gemini using an Atlas S2 CCD detector and mirror-collimated Cu-Kα radiation from a micro-focused X-ray tube and Bruker D8 Venture Photon CMOS diffractometer with an Incoatec microfocus sealed tube using Cu-*Kα* radiation. The data reduction, scaling and absorption correction were performed in CrysAlis PRO[25] and Apex3.[26]

The crystal structures were solved by charge-flipping methods in Superflip[27] and refined by full-matrix least-squares on F^2 values in Crystals.[28] All non-hydrogen atoms were refined anisotropically. Mercury[29] and Diamond 3.0[30] were used for structure visualization. The crystallographic data have been deposited in the Cambridge Crystallographic Data Centre as a supplementary publication. Melting points were measured on a hot stage microscope Kofler (KB T300) and were not corrected. Optical rotation was determined using an ADP 450 polarimeter (Bellingham-Stanley, USA) using 2 mL cuvettes. For the determination of the structures of **2** and **3**, the molecules were optimized using the Gaussian09[31] program, with B3LYP[32,33] as the functional and 6-31G(d) as a basis set. The vibrational analysis showed that both structures correspond to the local minima in the potential energy surface. The structures of the two complexes of **2** with naproxen were first optimized with B3LYP/6-31G(d), and their relative energy was then further specified using B3LYP/6-311G(d,p)++ and a D3 version of Grimme dispersion with Becke–Johnson damping,[34] added with the keyword *empiricaldispersion = gd3bj*.

Synthesis

(*S*)-3,5-dihydro-4*H*-dinaphtho[2,1-*d*:1′,2′-*f*][1,3]diazepin-4-one (1). To the stirred solution of (*S*)-1,1′-binaphthalene-2,2′-diamine **4** (0.284 g, 1 mmol) in pyridine (20 mL), triphosgene (0.1 g, 0.33 mmol) was added in small portions. The mixture was stirred overnight at the ambient temperature. The reaction mixture was partitioned between water and ethyl-acetate, and the pH of the mixture was adjusted to neutral by addition of HCl. The organic phase was washed with water (3 × 50 mL), dried with magnesium sulphate and evaporated to a volume of about 20 mL. The product precipitates from mother liqueurs as a white solid (0.155 g, 50%).

Melting point: over 310 °C

^{1}H NMR (DMSO-d_6) δ = 9.03 (s, 2H), 7.99 (dd, J = 12.0 Hz, J = 8.4 Hz, 2H), 7.45 (d, J = 8.8 Hz, 2H), 7.39 (t, J = 7.5 Hz, 2H), 7.20 (t, J = 7.7 Hz, 2H), 6.94 (d, J = 8.6 Hz, 2H).

^{13}C NMR (DMSO-d_6) δ = 165.9, 140.8, 131.7, 130.2, 129.2, 128.2, 126.2, 126.1, 124.6, 122.0, 121.9.

HRMS(*m*/*z*): calc. 311.1179, fd 311.1192 $[M + H]^+$

CCDC number: 2226943†

(*S*)-1,1′-Binaphthalene-2,2′-diisocyanate (5). Into a three-necked flask was placed the 20% solution of phosgene in toluene (2.7 mL, 5 mmol), more anhydrous toluene (5 mL) was added and the solution under a nitrogen atmosphere was placed into an ice bath. To (*S*)-1,1′-binaphthalene-2,2′-diamine **4** (0.284 g, 1 mmol) dissolved in anhydrous toluene (18 mL) was added anhydrous pyridine (1.4 mL, 17 mmol), and the mixture was cooled in an ice bath. Under the level of the phosgene solution, the cooled solution of (*S*)-1,1′-binaphthalene-2,2′-diamine was added. The reaction was stirred for 2 hours at 0 °C and for 3 hours at the ambient temperature. The mixture was then neutralized with 1 M HCl (12 mL), and the toluene layer was separated. The water layer was extracted with toluene (2 × 20 mL), and the organic layers were dried with calcium chloride. After filtration and evaporation, the product was obtained in the form of an orange oily liquid. Crude (*S*)-1,1′-binaphthalene-2,2′-diisocyanate was used in the following reactions without further purification.

^{1}H NMR ($CDCl_3$) δ = 8.01 (d, J = 8.7 Hz, 2H), 7.95 (d, J = 8.2 Hz, 2H), 7.50 (dd, J = 8.1, 6.9 Hz, 2H), 7.41 (d, J = 8.8 Hz, 2H), 7.34 (dd, J = 8.2 Hz, 6.2 Hz, 2H), 7.13 (d, J = 8.5 Hz, 2H).

^{13}C NMR ($CDCl_3$) δ = 133.1, 131.6, 120.8, 129.2, 128.6, 128.4, 128.1, 127.8, 126.3, 125.2, 123.5.

(*S*)-(−)-*N*-carboxybenzyl-1,1′-binaphthalene-2,2′-diamine (**6**)

(*S*)-(−)-1,1′-binaphthalene-2,2′-diamine **4** (1 g; 3.5 mmol) was dissolved in tetrahydrofuran (20 mL), and diisopropylethylamine (0.75 mL, 4.2 mmol, 1.2 equiv.) was added to the stirred solution. The mixture was cooled by the ice bath and benzyl chloroformate (0.53 mL; 3.5 mmol, 1 equiv.) was added dropwise. The reaction was stirred at ambient temperature for 1 hour upon TLC monitoring. Then water was added, and the mixture was extracted with dichloromethane (2 × 20 mL), organic layers were combined, washed with brine (20 mL) and dried by the addition of anhydrous magnesium sulphate. After filtration, the solution was concentrated *in vacuo*, and the crude product was purified by column chromatography (silica, hexane: ethyl acetate/6 : 1). After evaporation and drying, the product was obtained as white crystals in 45% yield.

Melting point: 156–158 °C

Optical rotation: $[\alpha]_D^{20} = -58^\circ$ (c = 1 M)

^{1}H NMR ($CDCl_3$) δ = 8.52 (d, J = 8.9 Hz, 1H), 8.01 (d, J = 9.1 Hz, 1H), 7.91 (d, J = 8.1 Hz, 1H), 7.85 (d, J = 8.8 Hz, 1H), 7.82 (d, J = 8.3 Hz, 1H), 7.40 (t, J = 7.4 Hz, 1H), 7.33–7.24 (m, 6H), 7.23 (dd, J = 5.1 Hz, 1.2 Hz, 1H), 7.19 (d, J = 6.9 Hz, 1H), 7.16 (d, J = 8.8 Hz, 1H), 7.13 (d, J = 8.5 Hz, 1H), 6.93 (d, J = 8.4 Hz, 1H), 6.62 (s, 1H), 5.07 (s, 2H).

^{13}C NMR ($CDCl_3$) δ = 153.7, 135.9, 134.9, 133.6, 132.5, 130.8, 130.4, 129.4, 128.55, 128.50, 128.3, 128.25, 128.24, 128.19, 127.3, 126.9, 125.2, 124.9, 123.7, 122.9, 119.7, 118.3, 66.9.

HRMS(m/z): calc. 441.1574, fd. 441.1573 $[M + Na]^+$

(*S*)-(−)-*N*-carboxybenzyl-1,1′-binaphthalene-2-amino-2′-isocyanate (7). Into a three-necked flask was placed protected binaphthalene diamine **6** (0.3 g, 0.72 mmol) dissolved in anhydrous toluene (5 mL), and anhydrous pyridine (0.5 mL, 6.1 mmol, 8.5 equiv.) was added. Under a nitrogen atmosphere, the mixture was cooled to 0 °C in an ice bath. Under the level of the solution, 20% solution of phosgene in toluene (0.75 mL, 1.4 mmol, 2 equiv.) was dropped by a syringe, and the mixture was stirred for 2 hours at 0 °C and a further 3 hours at ambient temperature. The reaction was neutralized by 1 M hydrochloric acid (2.5 mL), and the toluene layer was separated. The water layer was extracted with toluene (2 × 20 mL), and the organic layers were dried with $CaCl_2$. After filtration, the evaporation of the solvents gave crude **7** as a yellow oily liquid (100% yield assumed), which was used in the next steps without further purification.

^{1}H NMR ($CDCl_3$) δ = 8.52 (d, J = 9.0 Hz, 1H), 8.23 (d, J = 9.0 Hz, 1H), 8.07 (d, J = 9.3 Hz, 1H), 7.99 (d, J = 8.6 Hz, 1H), 7.93 (dd, J = 7.6 Hz, 3.9 Hz, 2H), 7.89–7.78 (m, 4H), 7.48 (ddd, J = 14.5 Hz, 6.7 Hz, 1.1 Hz, 2H), 7.40 (dd, J = 8.4 Hz, 4.0 Hz, 2H), 7.24 (d, J = 1.4 Hz, 1H), 6.93 (d, J = 7.7 Hz, 1H), 6.77 (d, J = 8.6 Hz, 1H), 6.25 (s, 1H), 5.08 (s, 2H).

^{13}C NMR ($CDCl_3$) δ = 153.8, 143.0, 137.0, 133.6, 132.6, 131.4, 130.4, 129.5, 128.6, 128.5, 128.3, 128.25, 128.24, 128.19, 127.9, 127.0, 125.5, 124.9, 123.3, 122.9, 119.7, 118.4, 67.0.

(*S*,*S*)-1,3-bis(2′-carboxybenzylamino-1,1′-binaphthalene-2-yl) urea (8). To (*S*)-(−)-*N*-carboxybenzyl-1,1′-binaphthalene-2-amino-2′-isocyanate (**7**, 0.72 mmol) dissolved in anhydrous toluene (40 mL), (*S*)-(−)-*N*-carboxybenzyl-1,1′-binaphthalene-2,2′-diamine (**6**, 0.3 g, 0.72 mmol) was added. The reaction mixture was stirred at 80 °C for 24 hours and monitored by TLC. The solvents were evaporated, and the crude product was chromatographed on a silica column (dichloromethane: ethyl acetate/30 : 1). The title compound was obtained as orange crystals in 82% yield.

Melting point: 120–122 °C

Optical rotation: $[\alpha]_D^{20} = -40^\circ$ (c = 1 M)

^{1}H NMR ($CDCl_3$) δ = 8.24 (d, J = 9.0 Hz, 2H), 8.00 (d, J = 9.0 Hz, 2H), 7.90 (dd, J = 16.5 Hz, 8.6 Hz, 4H), 7.83 (d, J = 19.5 Hz, 2H), 7.83 (s, 2H), 7.36 (dt, J = 31.6 Hz, 7.5 Hz, 4H), 7.29–7.22 (m, 6H), 7.21 (t, J = 7.6 Hz, 2H), 7.19–7.11 (m, 4H), 7.13–7.07 (m, 2H), 6.93 (d, J = 8.5 Hz, 2H), 6.79 (d, J = 8.5 Hz, 2H), 6.31 (s, 2H), 6.27 (s, 2H), 4.92 (s, 4H).

^{13}C NMR ($CDCl_3$) δ = 153.79, 152.65, 135.68, 135.14, 134.66, 132.46, 132.32, 130.80, 130.76, 130.10, 129.76, 128.46, 128.28, 128.20, 128.14, 128.09, 127.20, 125.23, 125.19, 124.78, 124.77, 121.24, 120.63, 120.01, 66.98.

HRMS(m/z): calc. 885.3047, fd. 885.3149 $[M + Na]^+$

(*S*,*S*)-1,3-bis(2′-amino-1,1′-binaphthalene-2-yl)urea (9). (*S*,*S*)-1,3-bis(2′-carboxybenzylamino-1,1′-binaphthalen-2-yl)urea (**8**, 0.5 g, 0.58 mmol) was dissolved in the mixture methanol: dichloromethane/12 : 3 (15 mL). Pd/C (10% wt) was added, and after evacuation the H_2 balloon was connected. The reaction mixture was stirred for 15 hours. After filtration over silica the solvent was evaporated, and the product was chromatographed on silica (dichloromethane: ethyl acetate/10 : 1). After evaporation, the product was obtained as yellow crystals in 95% yield.

Melting point: 250–252 °C

Optical rotation: $[\alpha]_D^{20} = -150^\circ$ (c = 1 M)

^{1}H NMR ($CDCl_3$) δ = 8.00 (d, J = 9.0 Hz, 2H), 7.86 (d, J = 8.1 Hz, 2H), 7.78 (d, J = 8.0 Hz, 2H), 7.68 (dd, J = 16.5 Hz, 8.9, 4H), 7.40 (t, J = 7.3 Hz, 2H), 7.29–7.18 (m, 8H), 7.14 (t, J = 7.3 Hz, 2H), 7.09 (d, J = 8.5 Hz, 2H), 6.80 (dd, J = 14.2 Hz, 8.6 Hz, 4H), 6.25 (s, 2H)

^{13}C NMR ($CDCl_3$) δ = 153.2, 142.4, 134.7, 133.6, 132.5, 130.9, 130.0, 129.3, 128.26, 128.18, 128.16, 127.1, 126.8, 125.3, 125.0, 123.6, 122.6, 121.4, 121.1, 118.0, 110.7.

HRMS(*m*/*z*): calc 594.2414, fd. 594.2433 $[M]^+$

(*S*,*S*)-tetranaphtho[1,2-*c*:1′,2′-*e*:1″,2″-*j*:1‴,2‴-*l*]-2,7,9,14-tetraaza cyclotetradecane-1,8-dione (2). (*S*)-1,1′-binaphthalene-2,2′-diamine (**4**, 0.284 g, 1 mmol) dissolved in anhydrous toluene (20 mL). (*S*)-1,1′-binaphthalene-2,2′-diisocyanate (**5**, 1 mmol) dissolved in anhydrous toluene (20 mL). A three-necked round-bottomed flask with anhydrous toluene (200 mL) was placed under a nitrogen atmosphere, and the prepared solutions were simultaneously added *via* a syringe pump at a rate of 1 mL h^{-1}. The reaction mixture was stirred at ambient temperature for 2 days. The solvents were evaporated, and the crude product was chromatographed on a silica column (dichloromethane: ethyl acetate/5 : 1). The evaporation gave the title compound as an amorphous white solid in 71% yield.

Melting point: 210–211 °C

Optical rotation: $[\alpha]_D^{20}$ = 857° (*c* = 1 M)

^{1}H NMR ($CDCl_3$) δ = 8.66 (d, *J* = 7.8 Hz, 2H), 7.97 (d, *J* = 8.1 Hz, 2H), 7.88 (d, *J* = 8.1 Hz, 4H), 7.76–7.59 (m, 2H), 7.39 (dd, *J* = 15.7 Hz, 6.7 Hz, 4H), 7.24–7.04 (m, 4H), 6.94 (s, 2H), 6.76 (d, *J* = 6.6 Hz, 4H), 6.10 (s, 2H), 5.51 (s, 2H).

^{13}C NMR ($CDCl_3$) δ = 152.7, 135.1, 133.1, 132.4, 132.4 130.1, 130.0, 129.9, 128.5, 127.1, 125.8, 124.6, 124.5, 123.8, 123.8, 119.3, 117.4.

MS(*m*/*z*): calc. 621.2285, fd. 621.2246 $[M + H]^+$

CCDC number: 2226944†

(*S*,*S*,*S*)-hexanaphtho[1,2-*c*:1′,2′-*e*:1″,2″-*j*:1‴,2‴-*l*:1⁗,2⁗-*q*:1′⁗,2′⁗-*s*]-2,7,9,14,16,21-hexaazacycloheneicosane-1,8,15-trione (3). (*S*,*S*)-1,3-bis(2′-amino-1,1′-binaphthalen-2-yl)urea (**9**, 0.285 g, 0.5 mmol) was dissolved in anhydrous toluene (20 mL). (*S*)-1,1′-binaphthalene-2,2′-diisocyanate (**5**, 0.142 g, 0.5 mmol) was dissolved in anhydrous toluene (20 mL). A three-necked round-bottomed flask with anhydrous toluene (200 mL) was placed under a nitrogen atmosphere, and the prepared solutions were simultaneously added *via* a syringe pump at a rate of 1 mL h^{-1}. The reaction mixture was stirred at ambient temperature for 2 days. The solvents were evaporated, and the crude product was chromatographed on a silica column (dichloromethane: ethyl acetate/20 : 1). The evaporation gave the title compound as an amorphous white solid in 52% yield.

Melting point: 223–225 °C

Optical rotation: $[\alpha]_D^{20}$ = −398° (*c* = 1 M)

^{1}H NMR ($CDCl_3$) δ = 7.89 (d, *J* = 8.2 Hz, 6H), 7.62 (d, *J* = 8.8 Hz, 6H), 7.41 (t, *J* = 7.5 Hz, 6H), 7.18 (t, *J* = 7.6 Hz, 6H), 7.07 (m, 6H), 6.89 (d, *J* = 8.5 Hz, 6H), 6.38 (s, 6H).

^{13}C NMR ($CDCl_3$) δ = 154.0, 134.5, 132.7, 131.3, 129.5, 128.2, 127.2, 125.6, 125.1, 124.6, 122.8.

HRMS(*m*/*z*): calc. 931.3391, fd. 931.3386 $[M + H]^+$

Conclusions

Binaphthalene-based cyclic homochiral ureas were synthesized by the targeted synthetic pathways, and their conformational properties in the solution and solid state were thoroughly tested. Compound **1**, where the urea moiety bridges one binaphthalene, adopts an unusual *cis*/*cis* conformation of urea protons. This feature stands behind the supramolecular oligomerization of **1**, rigidifying its crystals and preventing solubility in non-polar solvents. In the molecule of **2**, where two ureas bridge two binaphthalene moieties, a dynamic conformational behaviour occurs at the ambient temperature, which can be blocked at −30 °C. Despite the conformational mobility, this compound binds naproxen enantiomers and works as a chiral shifting agent for NMR, even at 25 °C. When three binaphthalene moieties are bridged with three ureas in compound **3**, a very flexible system is obtained. All the possible conformations are averaged here, and the switch between them is very quick. Naproxen is bound by this compound with unclear stoichiometry and negligible chiral solvating effect. The obtained results prove that cyclization of the molecule does not necessarily bring more rigid conformation, especially when strained structures are involved. Moreover, it sheds light on the mode of naproxen binding, where the interaction with both carbonyl and NH of the urea moiety is crucial.

Author contributions

RH-conceptualization, writing – editing, DJ-Investigation (synthesis), VE-investigation (X-ray), MJ-investigation (DFT), writing – editing, PC-investigation (NMR), writing – original draft, funding acquisition.

Conflicts of interest

There are no conflicts to declare.

Acknowledgements

This work was supported by the Czech Science Foundation grant number 20-07833S. Computational resources were supplied by the project "e-Infrastruktura CZ" (e-INFRA CZ LM2018140) supported by the Ministry of Education, Youth and Sports of the Czech Republic.

Notes and references

1 L. Pu, *1,1′-binaphthyl-based chiral materials: our journey*, Imperial College Press, 2009.
2 A. Shockravi, A. Javadi and E. Abouzari-Lotf, *RSC Adv.*, 2013, **3**, 6717.
3 T. L. Tarnowski and D. J. Cram, *J. Chem. Soc., Chem. Commun.*, 1976, **16**, 661.
4 R. C. Helgeson, K. Koga, J. M. Timko and D. J. Cram, *J. Am. Chem. Soc.*, 1973, **95**, 3021.
5 O. Rusin, K. Lang and V. Král, *Chem. – Eur. J.*, 2002, **8**, 655.
6 R. Holakovský, M. März and R. Cibulka, *Tetrahedron: Asymmetry*, 2015, **26**, 1328.

7 P. Cuřínová, M. Dračínský, M. Jakubec, M. Tlustý, K. Janků, P. Izák and R. Holakovský, *Chirality*, 2018, **30**, 798.
8 P. Cuřínová, P. Hájek, K. Janků and R. Holakovský, *Chirality*, 2019, **31**, 410.
9 M. Ricci and D. Passini, *Org. Biomol. Chem.*, 2003, **1**, 3261.
10 S. Colombo, C. Coluccini, M. Caricato, C. Gargiulli, G. Gattuso and D. Pasini, *Tetrahedron*, 2010, **66**, 4206.
11 M. Caricato, N. J. Leza, C. Gargiulli, G. Gattuso, D. Dondi and D. Passini, *Beilstein J. Org. Chem.*, 2012, **8**, 967.
12 V. Amendola, L. Fabbrizzi and L. Mosca, *Chem. Soc. Rev.*, 2010, **39**, 3889.
13 A. F. Li, J. H. Wang, F. Wang and Y. B. Jiang, *Chem. Soc. Rev.*, 2010, **39**, 3729.
14 A. Tejeda, A. I. Oliva, L. Simón, M. Grande, M. C. Caballero and J. R. Morán, *Tetrahedron Lett.*, 2000, **41**, 4563.
15 S. González, R. Peláez, F. Sanz, M. B. Jiménez, J. R. Morán and M. C. Caballero, *Org. Lett.*, 2006, **8**, 4679.
16 J. V. Hernández, A. I. Oliva, L. Simón, F. M. Muñiz, M. Grande and J. R. Morán, *Tetrahedron Lett.*, 2004, **45**, 4831.
17 K. M. K. Swamy, N. Jiten Singh, J. Yoo, S. K. Kwon, S.-Y. Chung, C.-H. Lee and J. Yoon, *J. Inclusion Phenom. Macrocyclic Chem.*, 2010, **66**, 107.
18 J. R. Loeffler, E. S. R. Ehmki, J. E. Fuchs and K. R. Liedl, *J. Comput.-Aided Mol. Des.*, 2016, **30**, 391.
19 M. Matsumura, A. Tanatani, I. Azumaya, H. Masu, D. Hashizume, H. Kagechika, A. Muranaka and M. Uchiyama, *Chem. Commun.*, 2013, **49**, 2290.
20 A. K. Hirose, *J. Inclusion Phenom. Macrocyclic Chem.*, 2001, **39**, 193.
21 P. Thordarson, *Chem. Soc. Rev.*, 2011, **40**, 1305.
22 The binding constants were calculated using the Bindfit application freely available at: **http://supramolecular.org**.
23 S. Goswami, S. Jana, S. Dey, D. Sen, H.-K. Fun and S. Chantrapromma, *Tetrahedron*, 2008, **64**, 6426.
24 I. Dąbkowska, J. Rak, M. Gutowski, J. M. Nilles, S. T. Stokes and K. H. Bowen, *J. Chem. Phys.*, 2004, **120**, 6064.
25 O. D. Rigaku, *CrysAlis PRO*, Rigaku Oxford Diffraction Ltd, Yarnton, Oxfordshire, England, 2020.
26 *Apex Bruker APEX3, SAINT*, Bruker AXS Inc., Madison, Wisconsin, USA, 2015.
27 L. Palatinus and G. Chapuis, *J. Appl. Crystallogr.*, 2007, **40**, 786.
28 *CRYSTALS*, Chemical Crystallography Laboratory, Oxford, 2011.
29 C. F. Macrae, I. J. Bruno, J. A. Chisholm, P. R. Edgington, P. McCabe, E. Pidcock, L. Rodriguez-Monge, R. Taylor, J. van de Streek and P. A. Wood, *J. Appl. Crystallogr.*, 2008, **41**, 466.
30 K. Brandenburg, *DIAMOND, Crystal Impact GbR*, Germany.
31 M. J. Frisch, G. W. Trucks, H. B. Schlegel, G. E. Scuseria, M. A. Robb, J. R. Cheeseman, G. Scalmani, V. Barone, B. Mennucci, G. A. Petersson, H. Nakatsuji, M. Caricato, X. Li, H. P. Hratchian, A. F. Izmaylov, J. Bloino, G. Zheng, J. L. Sonnenberg, M. Hada, M. Ehara, K. Toyota, R. Fukuda, J. Hasegawa, M. Ishida, T. Nakajima, Y. Honda, O. Kitao, H. Nakai, T. Vreven, J. A. J. Montgomery, J. E. Peralta, F. Ogliaro, M. Bearpark, J. J. Heyd, E. Brothers, K. N. Kudin, V. N. Staroverov, R. Kobayashi, J. Normand, K. Raghavachari, A. Rendell, J. C. Burant, S. S. Iyengar, J. Tomasi, M. Cossi, N. Rega, J. M. Millam, M. Klene, J. E. Knox, J. B. Cross, V. Bakken, C. Adamo, J. Jaramillo, R. Gomperts, R. E. Stratmann, O. Yazyev, A. J. Austin, R. Cammi, C. Pomelli, J. W. Ochterski, R. L. Martin, K. Morokuma, V. G. Zakrzewski, G. A. Voth, P. Salvador, J. J. Dannenberg, S. Dapprich, A. D. Daniels, Ö. Farkas, J. B. Foresman, J. V. Ortiz, J. Cioslowski and D. J. Fox, *Gaussian 09, Revision A.02*, Gaussian Inc., Wallingford, CT, 2009.
32 A. D. Becke, *J. Chem. Phys.*, 1993, **98**, 5648.
33 J. P. Perdew and Y. Wang, *Phys. Rev. B: Condens. Matter Mater. Phys.*, 1992, **45**, 13244.
34 S. Grimme, S. Ehrlich and L. Goerigk, *J. Comput. Chem.*, 2011, **32**, 1456.